Emergence of $p(2\times2)$ on highly doped *n*-type Si(100) surfaces: A scanning tunneling microscopy and spectroscopy study

Keisuke Sagisaka* and Daisuke Fujita
Nanomaterials Laboratory, National Institute for Materials Science, 1-2-1 Sengen Tsukuba, Ibaraki 305-0047, Japan
(Received 21 September 2004; revised manuscript received 16 February 2005; published 22 June 2005)

Scanning tunneling microscopy (STM) and spectroscopy were used to study the structural change between $c(4\times2)$ and $p(2\times2)$ on highly doped *n*-type Si(100) surfaces at 6 K. Sample voltage control during STM imaging allowed us to manipulate the surface structure between $c(4\times2)$ and $p(2\times2)$. We found that the sample voltage for producing $p(2\times2)$ [$c(4\times2)$] depends upon the tip-sample distance and dopant concentration. Coinciding with that, energy shifts of the π^* (π) state in tunneling spectra were observed. These results suggest that the structural change caused through STM was due to electron (hole) injection into the π^* (π) state. Also, the difference in how the $c(4\times2)$ and $p(2\times2)$ domains emerge, when electrons or holes are injected into the surface, can be understood by considering the electronic features of the π and π^* states.

DOI: 10.1103/PhysRevB.71.245319 PACS number(s): 68.35.Bs, 68.37.Ef, 68.47.Fg, 73.20.At

I. INTRODUCTION

The reconstruction of the Si(100) surface at room temperature (RT) is widely known as a relatively simple 2×1 dimer structure. The 2×1 periodicity is due to the thermally activated flip-flop motion of asymmetric dimers.[1] When the surface is cooled to below 200 K, the flip-flop motion is frozen and buckled dimers are observed.[2] Accordingly, the buckled dimers form two possible periodic arrangements: $c(4\times2)$ or $p(2\times2)$ [Fig. 1(i)]. Theoretical calculations have revealed that the energy of the $c(4\times2)$ structure is a few meV lower than that of the $p(2\times2)$ one.[3] Therefore $c(4\times2)$ has been accepted as the ground state structure of the Si(100) surface, which is consistent with the experimental observation down to 65 K.[4–6] However, recent studies using scanning tunneling microscopy (STM) and low energy electron diffraction (LEED) have challenged the ground state model and suggest phase transitions to the $p(2\times2)$ surface[7,8] or the flip-flop dimers[9,10] below 40 K.

The $p(2\times2)$ structure observed by STM around the liquid N_2 temperature (77 K) consists of fractions in association with defects, while $c(4\times2)$ is predominant. However, Hata *et al.* observed a single phase of $p(2\times2)$ on an *n*-type sample at 9 K by STM and suggested that the surface phase transition between $c(4\times2)$ and $p(2\times2)$ occurs around 40 K.[7] Their subsequent study suggested that the $c(4\times2)$ structure appeared at 5 K due to the tip-surface interaction.[8] On the other hand, Matsumoto *et al.* detected by LEED a rapid decrease in the intensity of the quarter-order diffraction spots below 40 K.[10] They interpreted the result as the phase transition from the ordered surface of $c(4\times2)$ to the disordered surface, which supported the STM observation of the flip-flop dimers at 5 K.[9]

Previously, we reported that the emergence of $p(2\times2)$ and the flip-flop dimers at 4.2 K is generated by an STM scan and is not the intrinsic nature of the Si(100) surface.[11,12] We suggested that tunneling electron injection plays a role in the surface phase modification. From such a finding, we concluded that the most stable configuration of the Si(100) surface is $c(4\times2)$ even at low temperature near liquid He. Also, the interesting nature of the Si(100) surface that develops at low temperature can explain the above controversial experimental results.[7–10]

In this paper, we present more extensive STM results concerning phase manipulation on the Si(100) surface, which give a better understanding of the emergence of $p(2\times2)$. We find a correlation between the sample voltage that induces the $p(2\times2)$ structure and the energy position of the empty dangling bond state in tunneling spectra, which suggests that $p(2\times2)$ is induced by tunneling electron injection into the

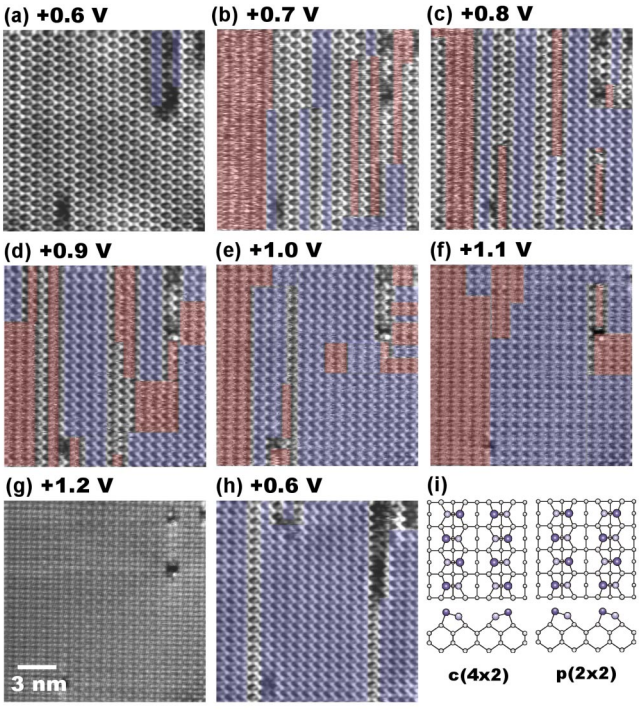

FIG. 1. (Color online) A series of empty state images of the Si(100) surface recorded with an increasing sample voltage at 6 K. The $p(2\times2)$ region (blue) and the flip-flop dimers (red) are colored for viewing. Sample: 0.01 Ω cm, $I=0.5$ nA.

upper part of the π^* state. The $c(4\times2)$ surface is recovered when carriers (electrons or holes) are injected into electronic states other than the π^* state. The mechanism for the emergence of $p(2\times2)$ is well explained by considering the quasi-one-dimensional electronic nature of the π^* states localized within the bulk band gap and the theoretically predicted charging effect.[13,14]

II. EXPERIMENT

We performed the STM observations in an ultrahigh vacuum (UHV) chamber with a base pressure of $<3\times10^{-9}$ Pa. All STM images and scanning tunneling spectroscopy (STS) data were acquired with electrochemically etched tungsten tips. Each tungsten tip was cleaned by electron-beam bombardment prior to use. The tip reliability for the STS data was confirmed by also using platinum-coated tungsten tips. Both tips provided almost the same spectrum features, although slight energy shifts in the spectra were observed when using different tips. STS and dI/dV imaging were applied by using a lock-in amplifier with modulation voltages of 10–20 mV and frequencies of 5–9 kHz. We used highly doped *n*-type Si(100) samples of two different resistivities (0.01 and 0.001 Ω cm at RT). The samples were degassed overnight in UHV and flashed to 1200 K for 10 s to obtain clean surfaces.

III. RESULTS AND DISCUSSION

A. Conditions for the emergence of $p(2\times2)$

Figure 1 shows how the $p(2\times2)$ surface grew as the sample voltage increased. The initial surface [Fig. 1(a)] was dominated by the $c(4\times2)$ structure and only fractions of the $p(2\times2)$ structure were observed (in the upper right of the image). When the surface was scanned below $V=+0.7$ V, no structural anomalies were observed. When the sample voltage was raised to above $V=+0.7$ V, the flip-flop motion of dimers was observed to start and then the dimers tended to stabilize in the $p(2\times2)$ arrangement. The phase change was observed to happen dimer row by dimer row. The phase transition efficiency rose as higher sample voltages were applied. However, the effect of $V=+0.7$ and +0.8 V was not enough to change the entire scanned area. Even several scans with such intermediate voltages led to only partial dimer rows of the $p(2\times2)$ phase. The largest areas of $p(2\times2)$ emerged when the surface was scanned at $V=+1.0$ or +1.1 V. The sample voltage above $V=+1.2$ V provided an image of a symmetriclike structure [Fig. 1(g)], which is known to not reflect the buckled dimer structure.[5,15] Thus the surface phase was not recognizable above $V=+1.2$ V. The effect of a high voltage scan on the surface structure, where flip-flop dimers or the symmetric image make it difficult to evaluate the composition, can be indirectly confirmed by decreasing the sample voltage to image a static surface after applying the sample voltage to be tested. For instance, Fig. 1(h) was recorded with $V=+0.6$ V just after the surface was scanned at $V=+1.2$ V [Fig. 1(g)]. Comparing Figs. 1(a) and 1(h), we can clearly see that the high voltage scan transformed the initial $c(4\times2)$ surface to a $p(2\times2)$ predominant surface. The flip-flop motion stopped at $V=+0.6$ V and the transformed surface formed by $V=+1.2$ V was retained.

We investigated the response of the Si(100) surface to different sample voltage as a function of the set current for two different dopant concentration samples. Figure 2 shows domain populations of $c(4\times2)$, $p(2\times2)$, and flip-flop dimers. These were counted from images recorded with various sample voltages, similar to those in Fig. 1 but with a larger area (30×30 nm). All data in Fig. 2 reflect a tendency similar to that described above: the population of $p(2\times2)$ increased as the voltage was raised while that of $c(4\times2)$ decreased. For the 0.01 Ω cm sample, the voltage dependence shifted toward a higher voltage when the set current increased [Fig. 2(a)]. In contrast, the voltage dependence for 0.001 Ω cm appeared at a lower voltage than that for 0.01 Ω cm, and showed only a slight shift as the set current increased [Fig. 2(b)]. The same experimental procedures were repeated for several samples using different tips and the same tendencies were observed. However, the tip quality affected the absolute position of the dependence curve with respect to the sample voltage, and its influence was more prominent for the 0.01 Ω cm sample.

The results in Fig. 2 provide much information on the emergence of the $p(2\times2)$ phase. The voltage dependences in Fig. 2(a) can immediately answer a question that arose in our previous study: why did the phase transition from $c(4\times2)$ to $p(2\times2)$ occur when the set current was decreased at a constant voltage?[11] The answer is that the threshold voltage needed to induce the flip-flop motion and $p(2\times2)$ for the 0.01 Ω cm sample depends greatly on the set current. As an extreme example, when the surface is scanned with $V=+0.8$ V and $I=5.0$ nA, the $c(4\times2)$ dominant surface is observed to be stable. Keeping $V=+0.8$ V and decreasing the tunneling current to 0.05 nA causes $p(2\times2)$ and flip-flop dimers to appear. Disagreement between the results of Fig. 2 and those in our previous experiments[11] regarding the combination of voltage and current quantities was probably due to the tip apex quality. During STM observation, the tip quality sometimes fluctuates. We noticed that such an occurrence varied the tip-sample separation and changed the threshold voltage for producing $p(2\times2)$. Since the quality of the tip apex is difficult to specify, we cannot discuss any further the influence of the tip upon the voltage dependence of the phase manipulation, but this will not affect our discussion below.

Yoshida *et al.* stated that there is an intrinsic phase transition from $c(4\times2)$ to $p(2\times2)$ below 40 K, and interpreted the $c(4\times2)$ phase observed with a low sample voltage at 5 K as a structure induced by the tip-sample interaction.[8] As shown in Fig. 2, the $p(2\times2)$ phase appeared when we increased the sample voltage (for both 0.01 and 0.001 Ω cm) or decreased the tunneling current (for 0.01 Ω cm). They interpreted the effects of change in the STM parameters (sample voltage and tunneling current) upon the structural change as a decrease in the tip-sample interaction. However, Fig. 1(h) reveals that such a probe effect does not happen. We confirmed that, as long as the surface was kept scanned at or below $V=+0.6$ V, no change in the surface structure occurred, although a voltage that was too low sometimes ruined the tip apex.

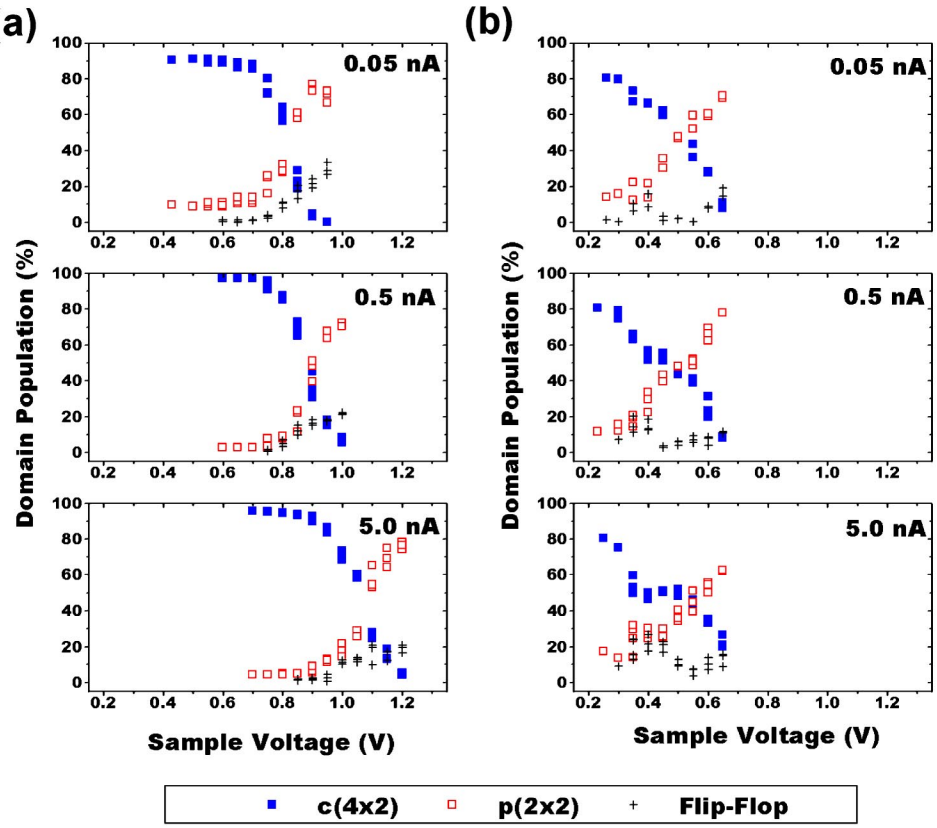

FIG. 2. (Color online) Domain populations of $c(4\times2)$ (filled square), $p(2\times2)$ (open square), and flip-flop dimers (cross) as a function of the sample voltage. Sample: (a) 0.01 Ω cm and (b) 0.001 Ω cm. The domain populations were counted from STM images of 30×30 nm areas recorded at various sample voltages with three different set currents. The STM imaging was done at 6 K.

Similar structure manipulation was recently done on the Ge(100) surface.[16–18] Phenomena common to both the Si(100) and Ge(100) surfaces were that $p(2\times2)$ [$c(4\times2)$] was produced when the surfaces were scanned with a positive (negative) sample voltage higher than a threshold. To explain the phase manipulation on a Ge(100) surface, Takagi *et al.* proposed a model based on electric field-dimer interaction.[18] Since an asymmetric dimer is characterized as a dipole due to charge transfer between the up and down atoms,[19] the polarity of a field applied to the dimer may influence the energy balance between $c(4\times2)$ and $p(2\times2)$. However, the electric field effect is not enough to explain the results of Fig. 2. In general, as the set current increases, the tip approaches the sample surface and the magnitude of the electric field increases between the tip and surface. Consequently, if the electric field induces the phase transition, a lower voltage would initiate it when a higher current is used. However, as the tip is closer to the surface, higher voltages are necessary to produce $p(2\times2)$ on the surface of a 0.01 Ω cm sample. In the case of 0.001 Ω cm, the tip-surface distance does not greatly influence the voltage dependence. It is unlikely expected that the dopant concentration of a substrate would affect the magnitude of the tip electric field applied to the dimers in the topmost surface. Therefore the electric field effect is unlikely to explain the behavior of the surface shown in Fig. 2.

Since there is a potential barrier of 0.1 to 0.2 eV for flipping a dimer,[20,21] a certain energy is needed to produce the $p(2\times2)$ domain. A plausible explanation for this is the inelastic scattering of tunneling electrons. However, the results of Fig. 2 show that a single effect of electron scattering upon the flip-flop motion is unlikely because the threshold voltage for the flip-flop motion should not be raised by an increase in the quantity of injected electrons or a decrease in the tip-sample separation. Furthermore, the effect of inelastic scattering is not apt to explain the difference in the voltage dependence between two samples with different dopant concentrations, unless the dopant concentration affects the energy barrier for the flip-flop motion. The estimated barrier height for flipping a dimer on Ge(100) is 0.3 to 0.4 eV,[22,23] whereas that on Si(100) is 0.1 to 0.2 eV.[20,21] Nevertheless, the threshold voltage is only 0.7 V for Ge(100),[16] which is equal to or even smaller than that for Si(100).

The flip-flop motion shown in Figs. 1(b)–1(f) seems to emerge because of fluctuation in the energy stability of dimers in between the $c(4\times2)$ and $p(2\times2)$ phases rather than because of simple excitation through the inelastic scattering process. If the flip-flop motion is caused solely by the inelastic scattering effect, when we scanned the surface with higher voltages [Figs. 1(d)–1(f)], more dimers should have been observed to flip-flop rather than $p(2\times2)$ becoming predominant. Although the inelastic process may cause the flip-flop motion when higher voltage ($V>+1.2$) is applied, we cannot accept that as the major mechanism for the emergence of $p(2\times2)$.

The voltage dependence of the phase manipulation correlates with the tip-sample separation and the resistivity of the substrate, so it is worth studying the surface electronic states and the effect of tip-induced band bending. Figure 3 shows the STS data acquired from the 0.01 and 0.001 Ω cm samples as a function of the set current. Every spectrum has three dominant features, which are consistent with the previ-

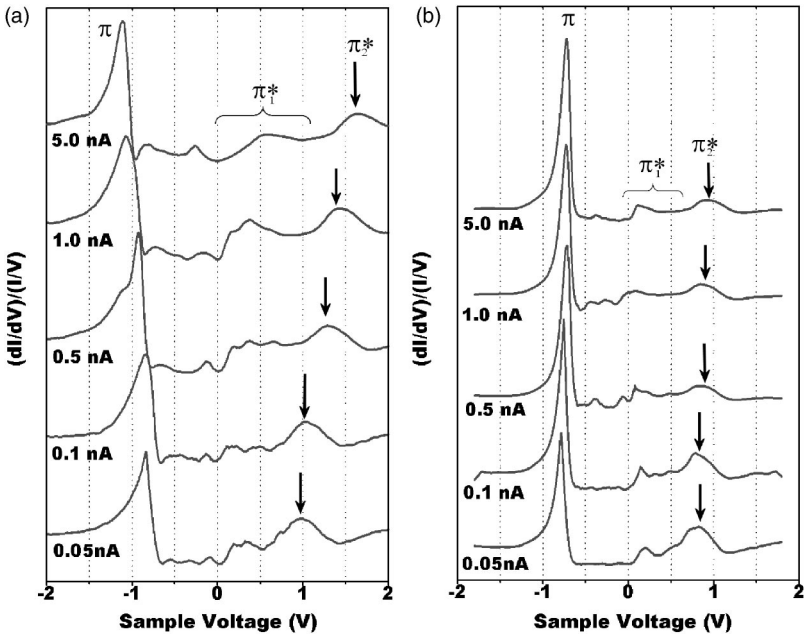

FIG. 3. Tunneling spectra at 6 K as a function of the set point current. Sample and set point voltage: (a) 0.01 Ω cm, $V=+1.1$ V, (b) 0.001 Ω cm, $V=+0.9$ V. $V_{pp}=20$ mV, $f=9$ kHz. The three major peaks are, respectively, denoted as π, π_1^*, and π_2^*.

ous results obtained at 80 K[24] and at room temperature.[25] These three peaks were previously assigned to π, π^* (π_1^*), and another branch of π^* states (π_2^*), respectively.[26,27] The origin of the second peak observed in the empty state, though, is still controversial. Since a symmetriclike structure, as seen in Fig. 1(g), is observed between the dimer rows and around the energy where the second peak is located, it has been suggested that the peak originates from unknown state(s) other than the dangling bond state.[24] However, an inverse photoemission spectroscopy measurement[29] has revealed only the dangling bond states in the energy region below 2.0 eV. Also, computational simulation using the electronic state of π_2^* can emulate the STM image of the symmetriclike structure between the dimer rows,[28] so we have adopted the electronic state of π_2^* as the assignment of the peak.

As shown in Fig. 3(a) (0.01 Ω cm sample), when the set current was above 0.1 nA, the peak shifts were observed in the π and π_2^* states. When the set current rose from 0.1 to 5.0 nA, the amount of energy shift in the position of the π peak was approximately 0.3 eV, whereas the π_2^* peak shifted by nearly 0.6 eV. The observed energy shifts were probably due to band bending induced by the tip electric field. The π_1^* state revealed a broad peak so its shift was difficult to confirm. The π_1^* state dispersed by approximately 0.9 eV and the upper part of it overlapped the π_2^* state.[3,27,30,31] Thus π_1^* was probably also affected by band bending when the current set point was changed. According to the results of a surface photovoltage (SPV) measurement on an *n*-type Si(100) surface (0.1 Ω cm),[32] the tip electric field bent the band upwards by ~0.6 eV when $V=+2.0$ V was applied and downwards by ~0.1 eV when $V=-2.0$ V. Since our observations were performed at a low temperature using a sample with a higher doping level, a quantitative comparison of the peak shifts in Fig. 3(a) to the SPV results is not appropriate. However, the tendency of band bending in Fig. 3(a)—a positive (negative) sample voltage revealing larger (smaller) band bending—is qualitatively in good agreement with the general nature of band bending on an *n*-type substrate, as observed through SPV measurement.[32] On the other hand, the 0.001 Ω cm sample did not show such energy shifts in the observed set current range [Fig. 3(b)]. Since the 0.001 Ω cm sample was a degenerate semiconductor,[33] its bulk conductance behaved like that of metal with decreasing temperature. Consequently, we would expect free carriers to effectively screen the electric fields in the surface even at the low temperature and prevent the peaks from shifting.

Comparing the results in Figs. 2 and 3, we find a correlation between the voltage dependence of the domain population of $p(2\times2)$ (Fig. 2) and the behavior of the band bending of the π_1^* and π_2^* peaks as a function of the set current (Fig. 3). For the 0.01 Ω cm sample, the domain population curve of $p(2\times2)$ as a function of sample voltage moved toward higher energy with an increasing tunneling current [Fig. 2(a)]. Similarly, the π_2^* peak in Fig. 3(a) shifted toward higher energy with an increasing set point current. (Here, we look at the π_2^* peak because its shift was easy to follow.) For 0.001 Ω cm, on the other hand, such shifts were not observed in either the domain population curve of $p(2\times2)$ [Fig. 2(b)] or the position of the π_2^* state [Fig. 3(b)]. These facts suggest that the emergence of $p(2\times2)$ was initiated by electron injection into the dangling bond state of the dimer. Since the upper edge of the π_1^* state overlaps the π_2^* state,[3,27,30,31] it is indefinite which state contributed more to the transition.

B. Transition yield from $c(4\times2)$ to $p(2\times2)$

To test the validity of our assumption that electron injection into the empty dangling bond state induces the emergence of $p(2\times2)$, we examined the transition yield against the sample voltage. Figure 4 shows empty state images of Si(100) recorded at the tested sample voltages (upper) and

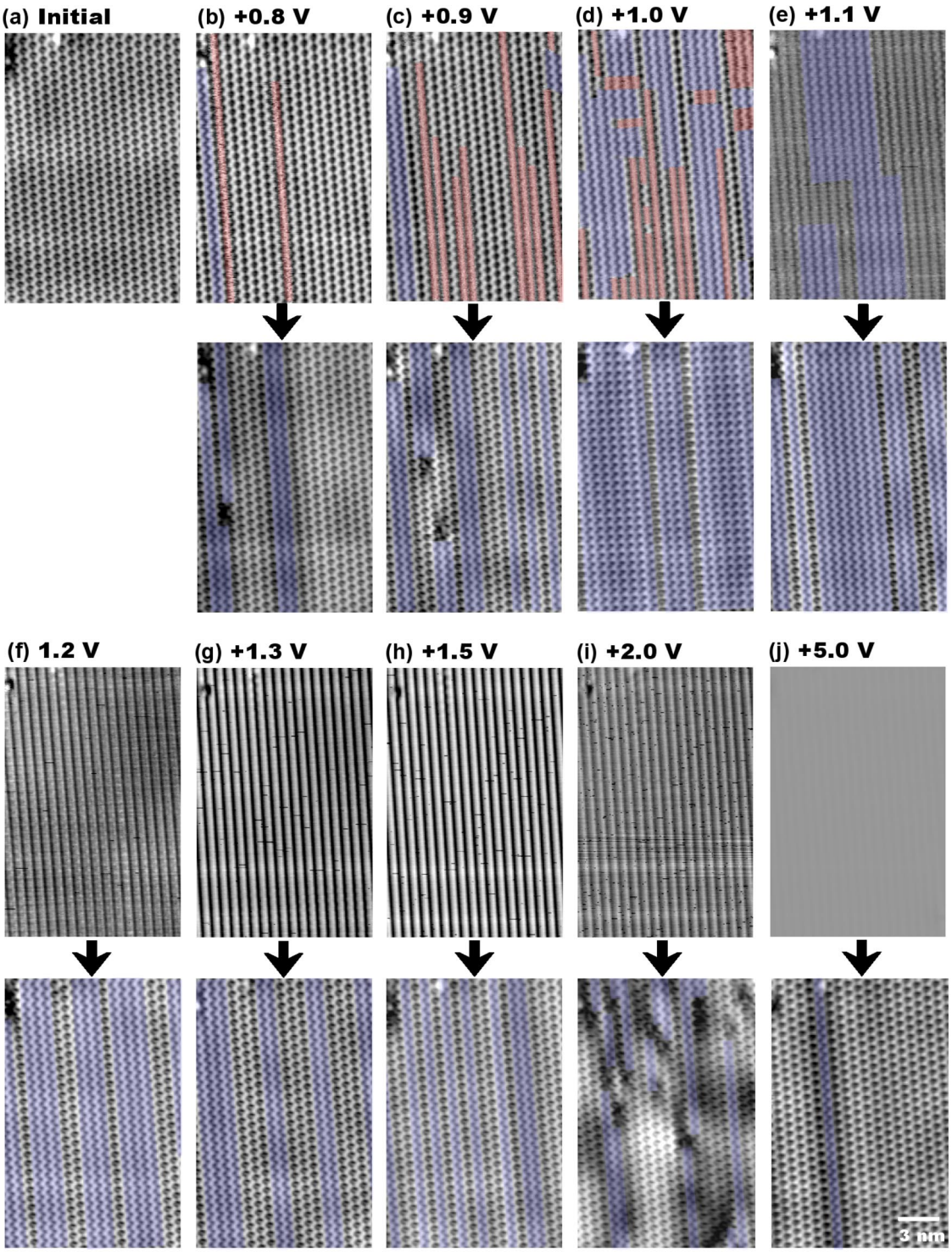

FIG. 4. (Color online) Empty state images of the Si(100) surface at 6 K during phase transition with different sample voltages (upper) and after the transition recorded at $V=+0.55$ V (lower). The $p(2\times2)$ region (blue) and the flip-flop dimers (red) are colored for viewing. Sample: 0.01 Ω cm, $I=0.5$ nA.

subsequent images recorded at $V=+0.55$ V (lower). The latter images of a static surface enabled us to confirm the consequence of using higher sample voltages to obtain the phase transition, as shown in Fig. 1(h). The tests were repeated within the same area, where the initial surface consisted of the $c(4\times2)$ structure [Fig. 4(a)]. The surface was initialized [restored to the $c(4\times2)$ surface] by scanning at $V=+5.0$ V before testing at each sample voltage. As shown in Fig. 4(j), this procedure can provide an almost perfect $c(4\times2)$ surface. In a range between $V=+0.8$ and $+1.1$ V [Figs. 4(b)–4(e), upper images], the flip-flop motion and the $p(2\times2)$ phase were observed, and the $p(2\times2)$ area increased as

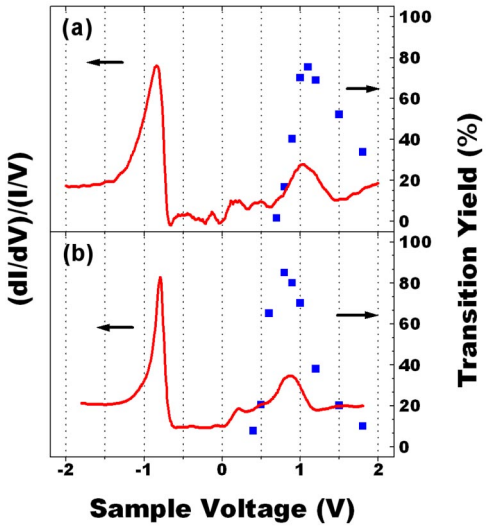

FIG. 5. (Color online) Tunneling spectra (solid line) and transition yields (filled square) from $c(4\times2)$ to $p(2\times2)$, as a function of sample voltage, at 6 K. The transition yield was evaluated as the rate of the $p(2\times2)$ area to the entire scanned surface of 29 $\times$29 nm. The area of $p(2\times2)$ was quantified from the image recorded at $V=+0.55$ V after the same surface was scanned with a tested sample voltage and $I=0.5$ nA. Sample: (a) 0.01 Ω cm and (b) 0.001 Ω cm.

we applied a greater voltage (lower images). For sample voltages of $V=+1.2$ and above, a symmetriclike structure appeared [Figs. 4(f)–4(j), upper images], and the $p(2\times2)$ area decreased as we increased the voltage (lower images).

We applied the same procedure to a larger area (29 $\times$29 nm) to qualitatively evaluate the transition yield. Here, the transition yield is defined as the ratio of the $p(2\times2)$ area to the entire scanned area, and the area of $p(2\times2)$ was estimated from the images recorded at $V=+0.55$ V after the tested sample voltage scan. Figure 5 shows the transition yield plotted against the sample voltage and the STS spectra for the 0.01 and 0.001 Ω cm samples. The results indicate that a specific sample voltage range is needed to transform the $c(4\times2)$ phase to the $p(2\times2)$ one. Furthermore, the range agrees with the peak of the π_2^* state. In accordance with the Fig. 2 results, as the set current increases, the yield curve for the 0.01 Ω cm sample shifted toward a higher energy.

The results in Figs. 4 and 5 again repudiate the possibility of the electric field affecting the emergence of $p(2\times2)$ (Ref. 18) and that of the tip-surface interaction affecting the emergence of $c(4\times2)$.[8] If the electric field induced the $p(2\times2)$ surface, the yield drop at higher voltage would not happen. Also, if the tip interaction was significant, the images at $V=+0.55$ V would not reveal different populations of $c(4\times2)$ and $p(2\times2)$. There is a possibility of flip-flop excitation caused by inelastic electron scattering at higher voltages, and accordingly this would prevent dimers in the electric field from stabilizing in $p(2\times2)$. However, the strong correlation between the yield curves and the tunneling spectra supports the model of electron injection into the upper edge of the π_1^* state or the π_2^* state causing the emergence of $p(2\times2)$.

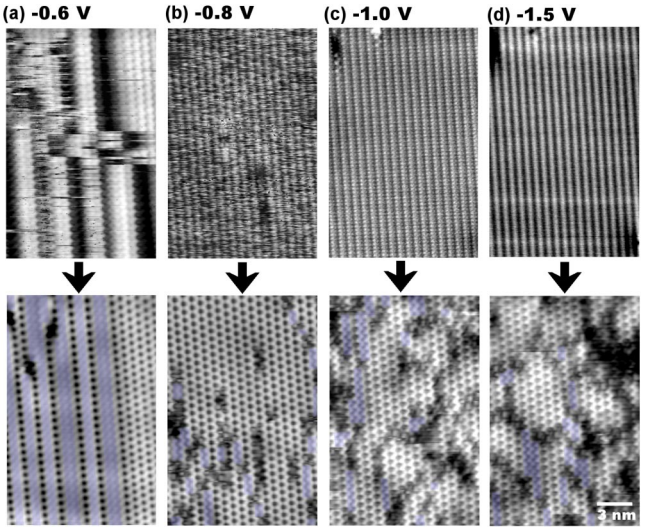

FIG. 6. (Color online) Filled state images of the Si(100) surface recorded with different sample voltages (upper) and subsequent images recorded at $V=+0.55$ V (lower). The $p(2\times2)$ regions are colored blue for viewing. Sample: 0.01 Ω cm, $I=0.5$ nA.

C. Effect of negative sample voltage scans upon the surface structure

The filled state image of a highly doped *n*-type Si(100) surface (<0.05 Ω cm) intricately varies with the sample voltage because the bottom of the π_1^* state is filled with electrons. As a result, the lower atom of an asymmetric dimer principally contributes to a low sample voltage image, while higher voltage images are determined by the ratio of tunneling electrons from between the upper and lower atoms. This is one reason that a structure that appears symmetric is observed in the filled state image. The details will be described elsewhere.[34] Figure 6 shows filled state images of the 0.01 Ω cm sample which were obtained with four different sample voltages (upper) and later images at $V=+0.55$ V (lower) to evaluate the influence of negative voltage scans upon the surface structure similar to Fig. 4. Before each negative voltage scan, the surface was initialized to a perfect $c(4\times2)$ phase by a single scan at $V=+5.0$ V. When the sample voltage was $V=-0.6$ V [Fig. 6(a)] or $V=-0.8$ V [Fig. 6(b)], the lower atoms of the asymmetric dimers were imaged (upper images). The symmetrical appearing dimers at $V=-1.0$ V [upper image of Fig. 6(c)] were not real symmetric dimers, but mostly asymmetric dimers and fractions of the flip-flop dimers, as we confirmed by dI/dV imaging (not shown). At a sample voltage greater than $V=-1.0$ V, both the upper and lower atoms contributed to the STM image, and some flip-flop dimers were generated, perhaps through the inelastic scattering process. Accordingly, a structure that appeared symmetric was imaged [Fig. 6(d)].

When the lower atoms were imaged with a low voltage scan ($V=-0.6$ V), the emergence of $p(2\times2)$ was observed, as was confirmed by the subsequent image at $V=+0.55$ V. The emergence of $p(2\times2)$ through a negative voltage scan is discussed in the next section. On the other hand, a higher negative voltage disrupted the ordered surface [Figs.

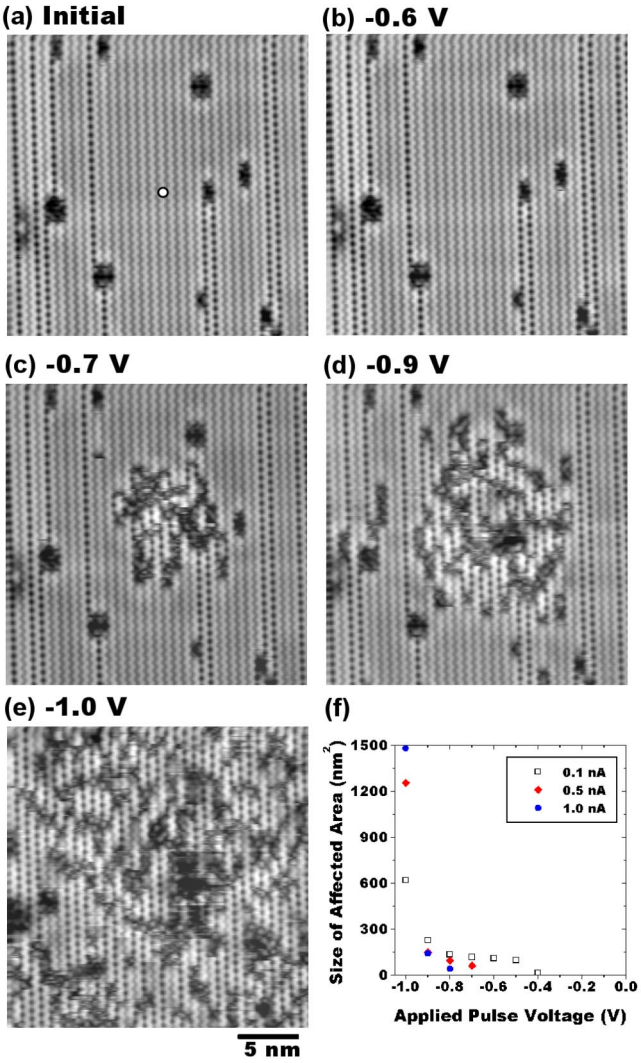

FIG. 7. (Color online) (a)–(e) Empty state images of the Si(100) surface at 6 K after negative pulse voltage (5-ms duration) was applied. All images were recorded at $V=+0.55$ V and $I=0.5$ nA after a pulse voltage of (b) −0.6 V, (c) −0.7 V, (d) −0.9 V, and (e) −1.0 V was applied to (a) the initial $p(2\times2)$ predominant surface. (f) The size of the affected area by a pulse voltage as a function of the applied pulse voltage for three set points. Sample: 0.01 Ω cm.

6(b)–6(d)]. Fractions of the $p(2\times2)$ areas and dark parts were observed in the lower images recorded at $V=+0.55$ V. The dark regions were not real defects but unstable dimers implanted between the $c(4\times2)$ phase and the $p(2\times2)$ one within a single dimer row. The disordered but $c(4\times2)$ predominant surface appeared after a single scan at $V<-0.8$ V in all cases, regardless of whether the initial surface was $c(4\times2)$ or $p(2\times2)$. Although we anticipated that the surface would flip-flop when scanned at $V=-0.8$ to −1.5 V, we could not precisely determine how the surface responded to the STM scan.

Figures 7(b)–7(e) show empty state images of the 0.01 Ω cm sample at $V=+0.6$ V after different negative pulse voltages lasting 5 ms were applied. The initial $p(2\times2)$ predominant surface [Fig. 7(a)] was made by a single scan with $V=+1.1$ V and $I=0.5$ nA. A pulse voltage $V=-0.6$ V or less did not affect the surface structure. When a pulse voltage of $V=-0.7$ V was applied at the image center [indicated by a dot in Fig. 7(a)], structural change was observed in an area of approximately 7×10 nm around the dimer where the pulse voltage was applied [Fig. 7(c)]. The affected area consisted of $c(4\times2)$ dimers and unstable dimers. As the pulse voltage increased, the influence of the pulse voltage expanded concentrically over the surface. Application of a pulse voltage beyond $V=-1.0$ V induced a disordered surface across an area of over 50×50 nm. Such an expansion is surprisingly large, compared to the result of the same experiment on Ge(100).[18] A 500-ms pulse voltage application of $V=-1.0$ V to the $p(2\times2)$ surface on Ge(100) induced a $c(4\times2)$ region of approximately 10×10 nm underneath the tip.[18] This deviation from the Si case may be related to the difference between Si and Ge in the barrier height for flipping dimers.

The minimum voltage that induces structural change also varied with the tip-sample distance. Figure 7(f) shows the size of the affected area as a function of pulse voltage for different current set points. The minimum voltage that was effective for flipping dimers was $V=-0.4$ V for 0.1 nA, while it was $V=-0.8$ V for 1.0 nA. As the STM tip-sample distance became smaller, the minimum voltage increased. This result is again inconsistent with an electric field effect upon the structural change. Tip-sample interaction is also unlikely because the tip-sample distance was fixed during the pulse voltage application. When we considered the shift of the π state with the set point in the STS spectrum of Fig. 3(a), we found the same tendency. Therefore hole injection into the π state during pulse voltage application generates flipping dimers, which leads to the disordered surface. The same results were obtained after pulse voltage application to the $c(4\times2)$ surface. A negative voltage seemed to just excite the flip-flop motion rather than create a $c(4\times2)$ surface. However, the surface resumed the $c(4\times2)$ phase after the pulse voltage application because this phase is more stable than $p(2\times2)$. In the case of Ge(100),[18] hole injection into the π state formed the $c(4\times2)$ surface. Therefore hole injection into the π state may also play a role in creating $c(4\times2)$ on the Si(100) surface. However, the flip-flop motion is more easily excited or there is weaker ordering on Si(100), so we could not reliably confirm this effect.

D. Emergence of $p(2\times2)$ in the filled state

A low negative voltage scan caused a $p(2\times2)$ surface to emerge when holes were injected into the bottom of the π_1^* state [Fig. 6(a)]. This did not happen on a low-doped sample (>0.05 Ω cm) or a *p*-type sample for which the Fermi energy does not cross the π_1^* state. Also, this manipulation is possible even at a higher temperature (~80 K) than that at which the $c(4\times2)\Rightarrow p(2\times2)$ manipulation is feasible when a positive sample voltage is applied (below 40 K). Figure 8 shows sequential images observed from the 0.01 Ω cm sample at 79 K as the sample voltage was changed [from (a) to (d)]. The initial image at $V=+0.3$ V was the $c(4\times2)$ predominant surface. We then applied a negative sample voltage. At $V=-0.9$ V [Fig. 8(b)], some dimers appeared to be

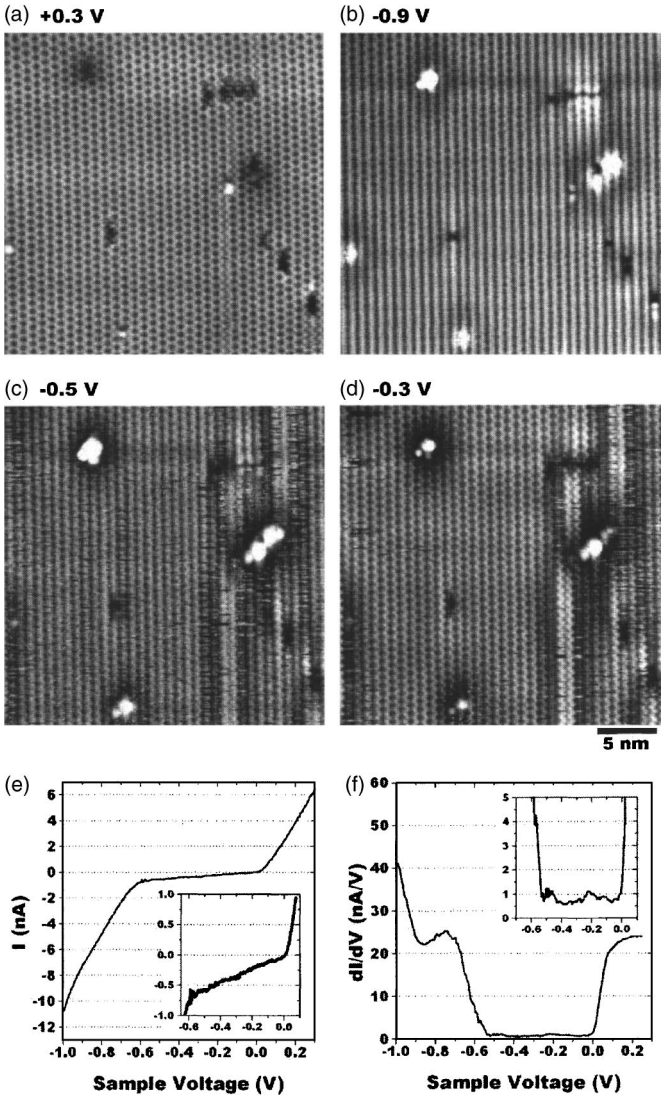

FIG. 8. (a) Empty and (b)–(d) filled state images of the Si(100) surface at 79 K recorded with sample voltages of (a) +0.3 V, (b) −0.9 V, (c) −0.5 V, and (d) −0.3 V, where $I=0.3$ nA. (e) Current and (f) differential conductance curves of the same surface as a function of the sample voltage. Set point: $V=-0.3$ V, $I=0.3$ nA. $V_{pp}=10$ mV, $f=5$ kHz. Sample: 0.01 Ω cm. The insets display an enlarged area around a low voltage range.

symmetric but the surface was still dominated by $c(4\times2)$. When the sample voltage was set in the range $V=-0.3$ to -0.6 V, the dimers over the scanned surface became unstable. Particularly in the region on the right side of the image, the $p(2\times2)$ structures were observed [Fig. 8(c)]. Furthermore, with a smaller sample voltage ($V<-0.3$ V), the dimers were again stabilized. As a result, the newly appearing $p(2\times2)$ structures remained [Fig. 8(d)]. Figures 8(e) and 8(d) are plots of current and differential conductance as a function of the sample voltage, obtained from the same sample at 79 K. We confirmed by dI/dV imaging that the π_1^* state extended down to approximately $V=-0.2$ V for this sample and the surface band gap approximately ranged from $V=-0.3$ to -0.5 V. These values were shifted by the band bending as we varied the set point (the tip-sample distance).

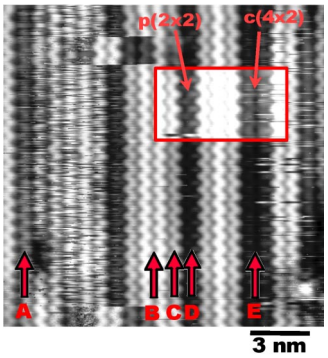

FIG. 9. (Color online) Filled state image of the Si(100) surface at 79 K. $V=-0.3$ V, $I=0.5$ nA. Sample 0.001 Ω cm. Arrows A and E indicate the $c(4\times2)$ dimer rows, while arrows B–D indicate the $p(2\times2)$ rows. The brightness of the dimer image in the box has been adjusted to aid viewing of the structure.

The same features were basically observed at 6 K and also for the 0.001 Ω cm sample, but the absolute positions of the bottom of the π_1^* state and the surface band gap described above were different for the 0.01 Ω cm sample because of the decrease in bulk conductivity at lower temperature.

Figure 9 shows a filled state image observed at $V=-0.3$ V at 79 K where the down atoms were imaged. Noted that the emergence of $p(2\times2)$ was induced dimer row by dimer row and each dimer row showed different conductance at this voltage. For instance, the two dimer rows indicated by arrow B were the brightest or the most conductive in the image, and dimer row D was the darkest or the least conductive. Dimer row C was moderately conductive. The most conductive dimer row always appeared in the $p(2\times2)$ phase, but the least conductive one could appear in either $c(4\times2)$ or $p(2\times2)$, as shown in the exaggerated inset of Fig. 9. Since dimer row B, C, and D were all arranged in the $p(2\times2)$ phase, the difference in conductivity was not due to electronic structure. It seems that the dimer rows aggregated in $p(2\times2)$ were metallic and the dimer rows on both sides of the aggregation were depleted. In the filled state imaging between the Fermi level and the valance band maximum, the conductivity was extremely low [Figs. 8(e) and 8(f)], where the electrons partially filling the π_1^* state were responsible for the tunnel current. Accordingly, we speculate that, to maintain the tunneling current as the applied voltage increased, some dimer rows improved their conductivity by consuming the carriers from neighboring dimer rows. If we assume that $p(2\times2)$ is more conductive along the dimer row than $c(4\times2)$, the surface is apt to become $p(2\times2)$ to improve the surface conductivity.

E. A model for the mechanism of phase transitions caused by STM

The results in Figs. 1–4 show that the $p(2\times2)$ phase appeared at 6 K when the surface was scanned with a particular range of positive sample voltage. Moreover, that voltage range varied with the tip-sample distance and sample resistivity. The similarity in the behavior of the shifts in the volt-

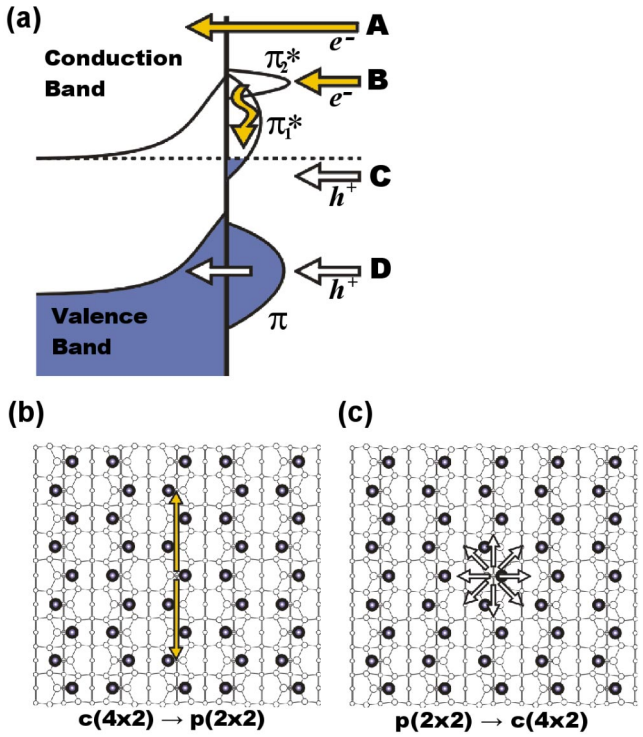

FIG. 10. (Color online) (a) Schematic band diagram showing tunneling processes with different sample voltages. Each process represents A: electron injection into the bulk conduction band, B: electron injection into the π_1^* and π_2^* states, C: hole injection into the filled π_1^* state, and D: hole injection into the π state. (b),(c) Schematic $p(2\times2)$ (b) and $c(4\times2)$ (c) surfaces showing the difference in the transport path of injected carriers.

age dependence of the domain populations (Fig. 2) and in the empty dangling bond states in the STS spectra (Fig. 3) with the tip-sample separation make it plausible that electron injection into the upper edge of the π_1^* or π_2^* states induced the emergence of $p(2\times2)$. On the other hand, the $c(4\times2)$ surface was recovered when the surface was scanned with a negative sample voltage corresponding to the energy of the π state or greater (Figs. 6 and 7). The minimum voltage that induced $c(4\times2)$ also shifted with the tip-sample distance, which agrees with the shift of the π state peak in STS as a function of the set point (Fig. 3). Moreover, a positive sample voltage higher than the energy of the π_2^* state (Fig. 4) was effective to create the $c(4\times2)$ surface. These findings are more plausibly explained by structural changes in association with the surface electronic state than by the tip-induced electric field or the tip-surface interaction.

Further evidence supporting the electronic state mechanism is the difference in the manner of domain growth between the two phases. The $p(2\times2)$ area developed with respect to each dimer row, as shown in Figs. 1 and 4. In fact, the expansion of the $p(2\times2)$ area propagated along the dimer row from the dimer beneath the STM tip, but it hardly diffused in the direction perpendicular to the dimer row. In contrast, concentric growth of $c(4\times2)$ from the dimer beneath the STM tip was observed, as shown in Fig. 7. The same tendency was reported on Ge(100) by Takagi *et al.*[18]

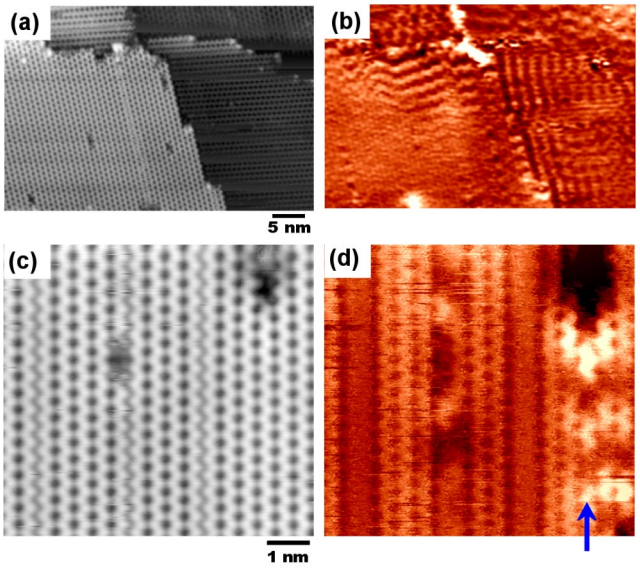

FIG. 11. (Color online) (a),(c) STM and (b),(d) corresponding dI/dV images of the Si(100) surface at 79 K. (a),(b) $V=+0.5$ V, $I=0.2$ nA, sample: 0.01 Ω cm, (c),(d) $V=+0.3$ V, $I=1.0$ nA, sample: 0.001 Ω cm. $V_{pp}=20$ mV, $f=5$ kHz.

Such a difference can be understood by considering the electronic structure of the Si(100) surface. Figure 10(a) depicts a schematic band diagram for the *n*-type Si(100) surface. The π_1^* state is located within the bulk band gap. Also, the bottom of the π_1^* state is partially filled, according to the STM observation. The dangling bond state of Si(100) has a dispersion along the dimer row.[29] Therefore the π_1^* state has a quasi-one-dimensional (1D) electronic feature. This was confirmed by our observation of standing waves. Figure 11 shows empty state images of the Si(100) surface [Figs. 11(a) and 11(c)] and simultaneously obtained dI/dV images [Figs. 11(b) and 11(d)]. The dI/dV images clearly reveal that standing waves emanated only along the dimer row direction from step edges [Fig. 11(b)] and a dimer vacancy [Fig. 11(d)], which acted as a potential barrier to scatter electron waves. This identification of standing waves was confirmed by the sample voltage dependence; i.e., the oscillation amplitude and wavelength varied with the sample voltage, in the same way as in STM observation on noble metals.[35,36] Here we stress that the strong oscillation along the dimer row indicated by an arrow in Fig. 11(d) retained the zigzag structure of the asymmetric dimer, which proves that the standing wave was derived from the π_1^* state. In contrast, standing waves were not observed in the filled state, which indicates that the π state overlapped the bulk valence band.

A comparison of these characteristics of the phase transition and electronic feature suggests four carrier injection processes [Fig. 10(a)]. Process B is electron injection into the upper edge of the π_1^* state and the π_2^* state. Injected electrons propagate along the dimer row through the π_1^* state [Fig. 10(b)] rather than being transported into the bulk conduction band. Consequently, the emergence of $p(2\times2)$ occurs through a change in buckling direction within a dimer row. On the other hand, holes injected into the π state (process D) diffuse concentrically in the surface through the bulk valance

band [Fig. 10(c)]. Such a transport process is consistent with the way $c(4\times2)$ appears in Fig. 7.

The most essential question, but a difficult one, is what mechanism directly induces the $p(2\times2)$ structure. In general, the $c(4\times2)$ phase has been understood to be the ground state structure because STM[2,4–6] and LEED[10] observation show that structure near the liquid N_2 temperature (77 K) and first principles calculation show that the $c(4\times2)$ energy is a few meV lower than that of $p(2\times2)$.[3] Our observations have proven this at lower temperatures as low as 670 mK.[37] One possible explanation for the emergence of $p(2\times2)$ is the charging effect. The influence of charge injection upon the surface structure was calculated by Nara *et al.*[13] and Seino *et al.*[14] They showed that negative charge (electron) injection into a dimer makes the energy of the $p(2\times2)$ structure lower than that of $c(4\times2)$. Also, the calculation by Nara *et al.* revealed that hole injection further stabilizes $c(4\times2)$,[13] while that by Seino *et al.* did not show hole injection having a prominent effect upon energy.[14] Their calculation results agree well with our observations. When electrons are injected into the π^* state, they flow along the dimer row or form standing waves. A dimer could feel negative charge and $p(2\times2)$ becomes more stable than $c(4\times2)$. When holes are injected into the π state, the flip-flop motion is induced. While the dimers are neutral or positively charged, $c(4\times2)$ is the most stable, so the surface is stabilized in the $c(4\times2)$ structure. Furthermore, electrons with higher energy than the π^* state mostly penetrate into the bulk conduction band (process A). In this case, the flip-flop excitation caused by inelastic scattering exceeds the charging effect, which prevents the $p(2\times2)$ phase from stabilizing.

However, the charging effect cannot explain all of our observation. The emergence of $p(2\times2)$ through a low negative voltage scan (process C) is induced by hole injection. Also, we question why electron injection into only the upper edge of the π_1^* state or the π_2^* state was effective for inducing $p(2\times2)$—why was a low voltage not effective? The best explanation we can currently offer is to assume that the dimers tend to transform into $p(2\times2)$ to improve local surface conductivity, as mentioned in the previous section. In both the electron and the hole injection cases, the $p(2\times2)$ phase appeared as the tunneling current increased with the sample voltage. Electrons or holes injected into the dimers are allowed to move only along the π_1^* band of the quasi-1D electronic feature until their energy is dissipated. Successive charge injection could augment the interaction among electrons in that state. The dimers may avoid such a situation by forming $p(2\times2)$. The dI/dV image in Fig. 11(d) shows that the boundary of the dimer rows in $p(2\times2)$ were vague while the dimer rows in $c(4\times2)$ were well resolved. This suggests that $p(2\times2)$ is rather two dimensional or bearing a transport channel in the direction perpendicular to the dimer row, which could relax the interaction among electrons. The mechanism of phase manipulation on Si(100) thus seems to include complex interactions among carriers and electronic states.

IV. CONCLUSION

We have characterized the structural changes between $c(4\times2)$ and $p(2\times2)$ on highly doped *n*-type Si(100) surfaces by STM at 6 K. In particular, we have studied conditions causing the emergence of $p(2\times2)$ by comparing the behavior of the phase transition and the location of the empty dangling bond states in tunneling spectra as a function of sample voltage and tunneling current (tip-sample distance). The sample voltage range needed to generate flip-flop dimers and produce $p(2\times2)$ depended upon the tip-sample separation and sample dopant concentrations. Similarly, the energy positions of π_1^* and π_2^* were determined by the tip-sample separation and sample dopant concentrations. From the correlation among these factors, we concluded that electron injection into the upper edge of the π_1^* state or the π_2^* state induces the $p(2\times2)$ phase. On the other hand, electron or hole injection into states other than the π^* states restored the $c(4\times2)$ surface. Previous calculations have shown that the $p(2\times2)$ becomes the ground state when the dimers are negatively charged. This prediction agrees with our experimental results.

The difference in the manner of domain growth between $c(4\times2)$ and $p(2\times2)$ can be explained by considering the transport paths of carriers injected by the STM tip. Since the π_1^* state has a quasi-1D localized electronic characteristic along the dimer row, injected electrons are transported in the dimer row instead of penetrating the bulk band. As a result, the emergence of $p(2\times2)$ happens collectively with respect to a dimer row. In contrast, the π state energetically overlaps the valence band and injected holes diffuse in the surface through that band. Accordingly, the recovery of the $c(4\times2)$ occurs rather concentrically over a wide range. The phase transition observed by STM is due to carrier injection into the filled and empty dangling bond states. The tip electric field influences the positions of these states relative to the Fermi level. Therefore the tip-surface distance and the dopant concentration of the sample affected the observation results. We did not observe any effect of physical tip-surface interaction upon the surface structure. The electric field may change the energy balance between $c(4\times2)$ and $p(2\times2)$, but we are not sure if it is detectable by STM.

ACKNOWLEDGMENT

We thank Jun Nara of the National Institute for Materials Science, Japan for his useful comments and discussion.

*Electronic address: sagisaka.keisuke@nims.go.jp

[1] R. J. Hamers, R. M. Tromp, and J. E. Demuth, Phys. Rev. B **34**, 5343 (1986).
[2] R. A. Wolkow, Phys. Rev. Lett. **68**, 2636 (1992).
[3] A. Ramstad, G. Brocks, and P. J. Kelly, Phys. Rev. B **51**, 14504 (1995).
[4] H. Tochihara, T. Amakusa, and M. Iwatsuki, Phys. Rev. B **50**, 12262 (1994).
[5] K. Hata, S. Yasuda, and H. Shigekawa, Phys. Rev. B **60**, 8164 (1999).
[6] T. Mitsui and K. Takayanagi, Phys. Rev. B **62**, R16251 (2000).
[7] K. Hata, S. Yoshida, and H. Shigekawa, Phys. Rev. Lett. **89**, 286104 (2002).
[8] S. Yoshida, T. Kimura, O. Takeuchi, K. Hata, H. Oigawa, T. Nagamura, H. Sakama, and H. Shigekawa, Phys. Rev. B **70**, 235411 (2004).
[9] T. Yokoyama and K. Takayanagi, Phys. Rev. B **61**, R5078 (2000).
[10] M. Matsumoto, K. Fukutani, and T. Okano, Phys. Rev. Lett. **90**, 106103 (2003).
[11] K. Sagisaka, D. Fujita, and G. Kido, Phys. Rev. Lett. **91**, 146103 (2003).
[12] K. Sagisaka, D. Fujita, G. Kido, and N. Koguchi, Surf. Sci. **566-568**, 767 (2004).
[13] J. Nara *et al.* (unpublished).
[14] K. Seino, W. G. Schmidt, and F. Bechstedt, Phys. Rev. Lett. **93**, 036101 (2004).
[15] X. R. Qin and M. G. Lagally, Phys. Rev. B **59**, 7293 (1999).
[16] Y. Takagi, Y. Yoshimoto, K. Nakatsuji, and F. Komori, J. Phys. Soc. Jpn. **72**, 2425 (2003).
[17] Y. Takagi, M. Yamada, K. Nakatsuji, and F. Komori, Appl. Phys. Lett. **87**, 1925 (2004).
[18] Y. Takagi, Y. Yoshimoto, K. Nakatsuji, and F. Komori, Surf. Sci. **559**, 1 (2004).
[19] D. J. Chadi, Phys. Rev. Lett. **43**, 43 (1979).
[20] K. Hata, Y. Sainoo, and H. Shigekawa, Phys. Rev. Lett. **86**, 3084 (2001).
[21] G. S. Hwang, Surf. Sci. **465**, L789 (2000).
[22] Y. Yoshimoto, Y. Nakamura, H. Kawai, M. Tsukada, and M. Nakayama, Phys. Rev. B **61**, 1965 (2000).
[23] H. Kawai, Y. Yoshimoto, H. Shima, Y. Nakamura, and M. Tsukada, J. Phys. Soc. Jpn. **71**, 2192 (2002).
[24] K. Hata, Y. Shibata, and H. Shigekawa, Phys. Rev. B **64**, 235310 (2001).
[25] J. J. Boland, Phys. Rev. Lett. **67**, 1539 (1991).
[26] H. Kageshima and M. Tsukada, Phys. Rev. B **46**, 6928 (1992).
[27] H. Okada, Y. Fujimoto, K. Endo, K. Hirose, and Y. Mori, Phys. Rev. B **63**, 195324 (2001).
[28] Y. Fujimoto, H. Okada, K. Endo, T. Ono, S. Tsukamoto, and K. Hirose, Mater. Trans., JIM **42**, 2247 (2001).
[29] L. S. O. Johansson and B. Reihl, Surf. Sci. **269/270**, 810 (1992).
[30] Z. Zhu, N. Shima, and M. Tsukada, Phys. Rev. B **40**, 11868 (1989).
[31] J. E. Northrup, Phys. Rev. B **47**, 10032 (1993).
[32] M. McEllistrem, G. Haase, D. Chen, and R. J. Hamers, Phys. Rev. Lett. **70**, 2471 (1993).
[33] S. M. Sze, *Semiconductor Devices, Physics and Technology*, 2nd ed. (Wiley, New York, 2001).
[34] K. Sagisaka and D. Fujita (unpublished).
[35] Y. Hasegawa and Ph. Avouris, Phys. Rev. Lett. **71**, 1071 (1993).
[36] M. F. Crommie, C. P. Lutz, and D. M. Eigler, Nature (London) **363**, 524 (1993).
[37] K. Sagisaka, M. Kitahara, D. Fujita, G. Kido, and N. Koguchi, Nanotechnology **15**, S375 (2004).